# Resonance poles in the complex-frequency domain for an oscillating barrier

R. Lefebvre*
*Laboratoire de Photophysique Moléculaire du CNRS, Université de Paris-Sud, 91405 Orsay, France and UFR de Physique Fondamentale et Appliquée, Université Pierre et Marie Curie, 75231 Paris, France*

N. Moiseyev†
*Department of Chemistry and Minerva Center for Non-linear Physics of Complex Systems, Technion-Israel Institute of Technology, Haifa 3200, Israel*
(Received 20 February 2004; published 14 June 2004)

The transmissivity calculated as a function of the frequency of oscillation for a particle meeting an oscillating barrier presents a resonant structure, as shown by Hagmann [Appl. Phys. Lett. **66**, 789 (1995)]. The origin of this structure is explained with the help of the expression giving the scattering amplitudes in the Floquet picture applied to a periodic Hamiltonian. It is possible to interpret it as due to the poles of the scattering amplitudes in the complex-frequency domain. For a moderate modulation amplitude the analysis makes use of the data obtained for the static barrier. The existence of these poles is not limited to the present model.

DOI: 10.1103/PhysRevA.69.062105 PACS number(s): 03.65.Xp, 72.20.Dp, 73.40.Gk

## I. INTRODUCTION

The scattering of a particle by an oscillating rectangular barrier is an interesting extension of the scattering by a static rectangular barrier which is treated in all textbooks of quantum mechanics (see, e.g., [1,2]). The oscillating barrier model has been used by Büttiker and Landauer [3,4] to propose an expression for the time it takes for a particle to tunnel through a barrier (see [5] for a review). Oscillating barriers of more general shapes have also been studied and shown to lead at high frequencies to resonances similar to those of a double barrier [6]. The oscillating barrier is considered as a good starting point to understand the mechanism of transmission through mesoscopic systems when there is a time-varying perturbation. A good example of such processes is photon-assisted tunneling in semiconductor structures with a multiple-quantum-well potential [7–9]. For a static potential the transmission is known to present a special profile when there are resonances associated with the system. This is the case for the double barrier, where the transmission reaches maxima on each resonance (unity for a symmetric potential). This resonance effect was first examined by Tsu and collaborators, both theoretically [10] and experimentally [11]. If a periodic perturbation is applied, one expects (and effectively finds) that each resonance splits into a number of satellites corresponding to the emission and absorption of quanta [12,13]. For a single barrier, there are still resonances, as shown in textbooks. They do not correspond to a leaking of quasibound states through barriers, but are the result of a constructive interference occurring above the barrier because of the reflections and transmissions taking place at each potential discontinuity. In the presence of a periodic perturbation one expects also that satellite features will be induced. This was shown [13] for a particle scattered by a rectangular barrier and interacting with an external oscillatory field, the interaction being written in the velocity gauge. Replicas of the over-barrier resonance structure are produced at energies below the barrier top, where no transmissivity is expected for a sufficiently thick barrier. The origin of these replicas is that, at these energies, absorption of a quantum raises the particle to one of the above-barrier resonances where transmission is facilitated. Hagmann [14] has recently developed a similar analysis for an oscillating barrier. Instead of studying the transmissivity profiles as a function of incident energy, he gave these profiles at fixed incident energy as a function of the frequency of oscillation. A resonant structure is observed, which has also its explanation in the mechanism of the replicas. The motivation now is the search for the frequencies which favor transmission. It is this structure which is the object of the present study. It will be shown to be related to the complex poles of the scattering amplitudes in the frequency plane.

After showing in Sec. II the procedure which is followed here to calculate the scattering amplitudes of the oscillating barrier, we analyze in detail in Sec. III the transmissivity profiles as a function of incident energy. The main result is that the pole in the energy plane associated with a replica has *exactly* the same imaginary part as the pole issued from the corresponding over-barrier resonance of the static barrier. Sec. IV presents transmissivity profiles at fixed incident energies below or above the top of the barrier. The profiles obtained below the top by Hagmann [14] are confirmed, with some additional structure due to the use of a larger amplitude of oscillation. A resonant structure can also be obtained above the top. For each case the positions of the maxima in the profiles are easily accounted for by a mechanism involving an absorption of quanta (below the top) or an emission of quanta (above the top). In Sec. V we indicate how we can derive expressions for the poles of the scattering amplitudes in the complex energy and frequency planes. We recall first how the scattering amplitudes can be written for a time-

*Electronic address: roland.lefebvre@ppm.u-psud.fr
†Electronic address: nimrod@techunix.technion.ac.il

 

dependent (but periodic) Hamiltonian [15,16]. This is the result of applying Floquet theory, with a special form given to the Green function displaying its dependence on resonance energies (or complex quasienergies) of the system. In Sec. VI a number of numerical experiments are described, each of them being corroborated by a proper use of the analytical expression of scattering amplitudes.

## II. CALCULATION OF SCATTERING AMPLITUDES

The wave equation (in atomic units) is

$$\left[-\frac{1}{2m}\frac{\partial^2}{\partial x^2}+V_0(x)+V_1(x)\cos(\omega t)\right]\Psi(x,t)=i\frac{\partial\Psi(x,t)}{\partial t}, \tag{1}$$

where $V_0(x)$ and $V_1(x)$ are constant (say, $V_0$ and $V_1$) when $-L/2\leqslant x\leqslant L/2$ and zero otherwise. For a barrier $V_0$ is positive. $L$ is the width of the barrier.

The solutions in the potential-free regions on the left and on the right of the barrier are simply combinations of free waves. Calling these sectors 1 and 3, we write the general solutions as

$$\Psi^{(1,3)}(x,t)=\sum_n \sqrt{\frac{m}{k_n^{(1,3)}}}t_n^{(1,3)}\exp[i(k_n^{(1,3)}x-E_nt)] + \sum_n \sqrt{\frac{m}{k_n^{(1,3)}}}r_n^{(1,3)}\exp[-i(k_n^{(1,3)}x+E_nt)], \tag{2}$$

with $k_n^{(1,3)}=[2mE_n]^{1/2}$ and $E_n=E+n\omega$. The energy $E$ can be identified with the incident energy of the particle. By mixing waves with different energies we are preparing the ground for a change in the number of quanta accompanying the particle when it meets the barrier. No assumption at this stage is made about boundary conditions. This is to be done later and is typical of the transfer matrix method [10,13,17] to be used here. The factors in front of the amplitudes simplify the calculation of transition probabilities (see below). It is to be noted that depending on $n$, the wave numbers $k_n^{(1,3)}$ can be either real ($E_n>0$) or imaginary ($E_n<0$). This defines the open or closed channels, respectively. For the latter, with a wave number of the form $k_n^{(1,3)}=i\kappa_n^{(1,3)}$, $\kappa_n^{(1,3)}>0$, all the waves associated with the $t_n^{(1)}$'s diverge for $x\to-\infty$ while those associated with the $r_n^{(3)}$'s diverge for $x\to+\infty$. Anticipating from boundary conditions to be made later, it is important to mention that among all amplitudes to be made zero are those associated with the diverging waves.

The solution in the middle sector with $-L/2\leqslant x\leqslant L/2$ (sector 2) has been given many times in the literature [14,18–20]. Its most general form is

$$\Psi^{(2)}(x,t)=\left\{\sum_n t_n^{(2)}\exp[i(k_n^{(2)}x-E_nt)]+\sum_n r_n^{(2)} \times\exp[-i(k_n^{(2)}x+E_nt)]\right\}\times\exp\left[-i\frac{V_1\sin(\omega t)}{\omega}\right], \tag{3}$$

where $k_n^{(2)}$ is $[2m(E_n-V_0)]^{1/2}$. The wave numbers can again be either real or imaginary, but all types of waves retain a meaning in the barrier region. The summation index $n$ present in all sectors is in practice limited to the range $-N\leqslant n\leqslant N$, where $N$ is the number of effectively gained or lost quanta. This number depends on the amplitude of oscillation $V_1$. The number of amplitudes $t$ or $r$ in each sector is therefore $2(2N+1)$. Matching at the sector boundaries is done by ensuring continuity of the wave function and of its derivative with respect to position. An additional matching is needed, since the wave functions depend on time. The time matching can be done either by identification of Fourier components [20,21] or more simply by identification of the functions at a set of $(2N+1)$ times within a period of the oscillation [14,22,23]. Starting from a set of amplitudes in sector 1 written as a column vector $\mathbf{a}^{(1)}$ made of all $t_n^{(1)}$ and $r_n^{(1)}$, we reach after two matching procedures sector 3 with its associated column vector $\mathbf{a}^{(3)}$ made of all $t_n^{(3)}$ and $r_n^{(3)}$. The relations between the two vectors has the form

$$\mathbf{a}^{(3)}=\mathcal{M}\mathbf{a}^{(1)}. \tag{4}$$

With the previous conventions the transfer matrix $\mathcal{M}$ is square and of dimensions $(4N+2)\times(4N+2)$. The scattering boundary conditions are now applied. In the vector $\mathbf{a}^{(1)}$ all the $t_n^{(1)}$ are made zero, except $t_0^{(1)}$ which is taken equal to unity. In the vector $\mathbf{a}^{(3)}$, all the amplitudes $r_n^{(3)}$ are taken equal to zero. There results a set of inhomogeneous relations determining all scattering amplitudes. With the normalization chosen for the waves in the asymptotic sectors 1 and 3, the scattering probabilities are simply the squared moduli of the amplitudes of the open channels in either sector 1 (reflection) or sector 3 (transmission). The total transmissivity $T(E)$ is $\Sigma_n|t_n^{(3)}|^2$, the sum over all open channels of the partial transmission probabilities.

## III. TRANSMISSIVITY PROFILES AT FIXED FREQUENCY

Our parameters for the barrier are the same as those of Hagmann [14]—that is, a width of 10 Å (or 19.90 a.u.) and a height of 11 eV (or 0.4042 a.u.). The mass of the particle is that of a free electron, $m=1$ a.u. In this preliminary study of tranmissivities as a function of incident energy we take $\omega$ equal to 5 eV (or 0.1837 a.u.). In order to amplify the effects to be analyzed we take a somewhat larger amplitude of oscillation than those of Hagmann [14]: $V_1=5$ eV instead of at most 0.055 eV. Figure 1 gives in the left panel the transmissivity of the static barrier. It has a well-known structure. Transmission starts when the energy gets close to the top of the barrier. Four resonances are displayed above the barrier, with the tranmissivity reaching the value unity, as expected. The right panel gives the total transmissivity of the oscillating barrier, with amplification below the barrier top. A maximum number of exchanged quanta, $N=5$, ensures convergence of the calculations. An interesting result of this calculation is that the oscillation has induced replicas of the over-barrier structure. Such replicas were previously observed and analyzed in a similar study [13], with the particle coupled to an external oscillatory electric field. The explana-

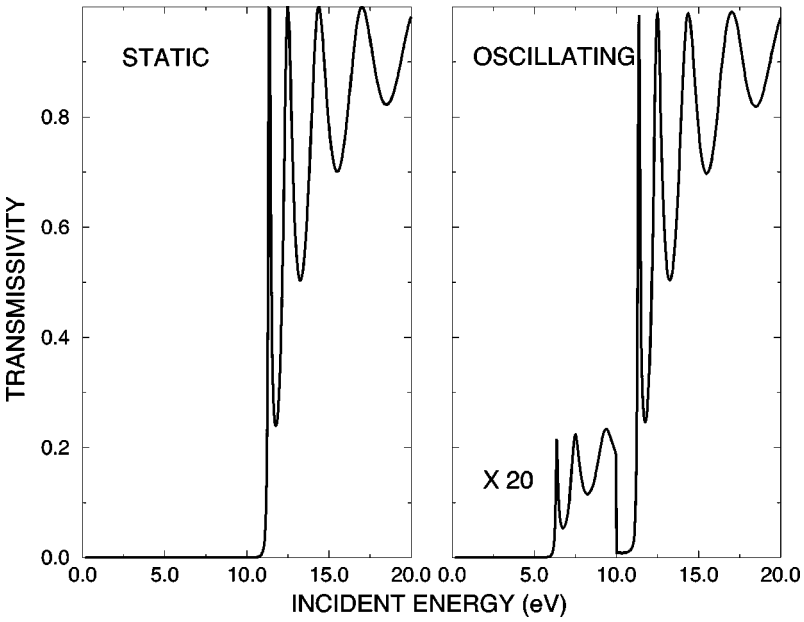


FIG. 1. Transmissivities as a function of incident energy for the static (left) and the oscillating barrier (right). In the latter case the total transmissivity $T(E)$ is given. The replica structure is amplified by a factor of 20. The replica phenomenon is due to an absorption of quanta allowing for a transmission mediated by the over-barrier resonances. Table I gives the numerical evidence supporting this analysis.

tion is very simple: by absorption of one quantum, the particle reaches the energy of one of the over-barrier resonances where transmission is a very efficient.

An additional insight into the meaning of replicas comes from a study of the poles of the scattering amplitudes. These poles in the complex energy plane are obtained by searching for the zeros of the inverse of these amplitudes. This is done from some trial value by a complex Newton-Raphson procedure. We have checked that, as predicted by the general theory [24], the pole can be obtained from any of the reflection or transmission amplitudes. All results presented in Table I for the static barrier have been obtained from the transmission amplitude and for the oscillating barrier from $t_0^{(3)}$—that is, the transmission amplitude with no net absorption or emission of quanta. The first four resonance energies of the static barrier are in column 1, those of the oscillating barrier in column 2. With the present amplitude of oscillation, the resonance shift is very small, as shown by a comparison of the real parts of the resonance energies. The interesting information is in column 3 giving the poles associated with the first four replicas. The real parts of the resonance energies are very precisely those of the over-barrier resonances minus one quantum (i.e., 5eV). Their imaginary parts are in coincidence. The conclusion which emerges is that each replica has the same width as the corresponding resonance issued from the static barrier. This is confirmed by the analysis of the next section, which will also be the basis for looking at poles in the complex frequency plane.

TABLE I. Poles of scattering amplitudes in the complex energy plane. First column: the poles associated with the first over-barrier resonances of the static barrier. Second column (a): the poles issued from these resonances when the barrier oscillates. Third column (b): the poles of the replicas. The replica of the fourth resonance is not seen in Fig. 1 because it interferes with the second over-barrier peak. The transmission amplitude which is used in the search of the poles for the oscillating barrier is that with no net absorption or emission of quanta that is, $t_0^{(3)}$. All energies are in eV.

| Static barrier | Oscillating barrier (a) | Oscillating barrier (b) |
|---|---|---|
| $11.3610-i0.08571$ | $11.3609-i0.08581$ | $6.3609-i0.08581$ |
| $12.4470-i0.3382$ | $12.4467-i0.3385$ | $7.4467-i0.3385$ |
| $14.2649-i0.7450$ | $14.2648-i0.7457$ | $9.2648-i0.7457$ |
| $16.8229-i1.2886$ | $16.8227-i1.2902$ | $11.8227-i1.2902$ |

## IV. TRANSMISSIVITY PROFILES AT FIXED INCIDENT ENERGY

We turn now to the study of transmissivity profiles for fixed incident energy and varying frequency. Two cases are examined: either an incident energy below the top of the barrier, $E_{inc}=10$ eV, or above the top, $E_{inc}=20$ eV. Figure 2 gives these two profiles. In both cases a resonance structure is present. The graph of the upper panel is similar to that given by Hagmann [14], although with a larger modulation amplitude there is an additional structure on the low-frequency side, corresponding to multiquantum processes. The first four peaks correspond to the addition of, respectively, four, three, two, and one quanta to the incident energy to reach the first over-barrier resonance, while the three humps which follow lead to the next three over-barrier resonances by absorption of one quantum. The graph of the lower panel has a similar explanation, but now in terms of emission of one quantum to reach the over-barrier resonances. This explanation in terms of multiquantum processes is also given in Table II, where the different frequencies corresponding to the various peaks or humps are related to the absorption or emission of a number of quanta allowing the access to one of the four above-barrier resonances. The two last columns give two estimates of the complex-frequency poles explaining the features of the transmissivity profiles. The column labeled "pole (num.)" gives the numerical estimates from the zeros of the inverse of an appropriate transition amplitude. The column labeled "pole (an.)" gives the

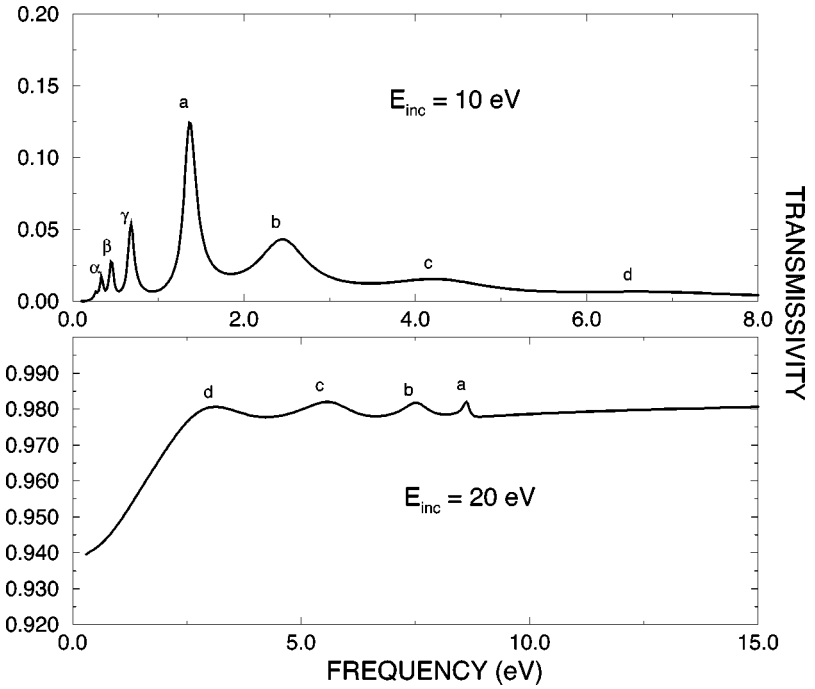


FIG. 2. Total transmissivities as a function of frequency (expressed in eV). Upper panel: with a fixed incident energy $E_{inc}$ equal to 10 eV, the peaks or humps correspond to the absorption of a number of quanta leading to the resonances associated with those of the static case. Table II gives the numerical evidence supporting this analysis. Lower panel: corresponding to an incident energy equal to 20 eV, the features are associated with the emission of one quantum to reach the first four over-barrier resonances, as shown also in Table II. In both cases the labeling refers to the frequencies listed in this table.

pole estimate from the analytical expressions derived below in Sec. V, using the primitive data collected in Table I.

## V. TIME-INDEPENDENT SCATTERING AMPLITUDES FOR TIME-DEPENDENT PERIODIC HAMILTONIANS

A very interesting aspect of Hamiltonians periodic in time is that many results about their wave functions are very similar to those obtained for time-independent Hamiltonians. Time plays the part of an additional dynamic variable. This means that the wave functions can be developed in an extended space obtained as the direct product of a basis in coordinate space by a complete set of square-integrable functions periodic in time. Time-independent transition probabilities can be defined between asymptotic states before and after a collision if the time-dependent term in the Hamiltonian vanishes in the asymptotic regions [15,16]. This is clearly the case for an oscillating barrier.

The solution of the time-dependent Schrödinger equation with continuum boundary conditions, according to Floquet theorem [25], can be written:

$$\Psi_E(x,t) = \exp[-iEt]\Phi_E(x,t), \tag{5}$$

with

TABLE II. Analysis of the transmissivity peaks as a function of the frequency of oscillation of the barrier. The upper part corresponds to an incident energy equal to 10 eV, the lower part to 20 eV. The label of each peak or feature in the profiles is given in column 1. The number of quanta needed to reach an over-barrier resonance by the absorption (upper part) or emission (lower part) of quanta is shown in column 2, with $n$ either positive (absorption) or negative (emission). The column labeled $\omega$ gives the frequencies associated with the maxima in the profiles. The column labeled $E_{inc}+n\omega$ shows evidence that one of the over-barrier resonances is reached by absorption or emission of quanta. The two last columns give the numerical and analytical estimates of the frequency poles explained in the text. Frequencies and energies are in eV.

| Label | $n$ | $\omega$ | $E_{inc}+n\omega$ | pole (num.) | pole (an.) |
|---|---|---|---|---|---|
| $\alpha$ | 4 | 0.3396 | 11.3584 | $0.3404-i0.02116$ | $0.3402-i0.02145$ |
| $\beta$ | 3 | 0.4594 | 11.3782 | $0.4542-i0.02860$ | $0.4536-i0.02860$ |
| $\gamma$ | 2 | 0.6841 | 11.3682 | $0.6801-i0.04266$ | $0.6805-i0.04291$ |
| $a$ | 1 | 1.372 | 11.3732 | $1.3599-i0.08567$ | $1.3609-i0.08581$ |
| $b$ | 1 | 2.4517 | 12.4517 | $2.4473-i0.3395$ | $2.4467-i0.3385$ |
| $c$ | 1 | 4.2044 | 14.2044 | $4.2658-i0.7462$ | $4.2648-i0.7457$ |
| $d$ | 1 | 6.5862 | 15.6852 | $6.8261-i1.2902$ | $6.8227-i1.2902$ |
| $a$ | −1 | 8.6204 | 11.3796 | $8.6391+i0.08579$ | $8.6391+i0.0858$ |
| $b$ | −1 | 7.5224 | 12.4276 | $7.5533+i0.3386$ | $7.5533+i0.3385$ |
| $c$ | −1 | 5.5704 | 14.4296 | $5.7347+i0.7444$ | $5.7352+i0.7457$ |
| $d$ | −1 | 3.1304 | 16.8696 | $3.1082+i1.2480$ | $3.1773+i1.2902$ |

$$\Phi_E(x,t+T)=\Phi_E(x,t). \tag{6}$$

$T$ is the period of the Hamiltonian. $\Phi_E(x,t)$ is an eigenfunction of the Floquet Hamiltonian:

$$H_F(x,t)=H(x,t)-i\frac{\partial}{\partial t} \tag{7}$$

according to

$$H_F(x,t)\Phi_E(x,t)=E\Phi_E(x,t). \tag{8}$$

The scattering solutions in the different sectors discussed in Sec. II were all of this form.

Consider now that before collision (i.e., before meeting the barrier) the particle is described in extended space by the wave function

$$\varphi_i(x,t)=\sqrt{\frac{m}{k_i}}\exp[ik_ix]\exp[-iE_it], \tag{9}$$

with $E_i=k_i^2/2m$. This form implies that the basis function in the time domain is unity. After the collision the wave function may become

$$\varphi_{f,n}(x,t)=\sqrt{\frac{m}{k_{f,n}}}\exp[ik_{f,n}x]\exp[-i(E_{f,n}-n\omega)t], \tag{10}$$

with $E_{f,n}=k_{f,n}^2/2m=E_i+n\omega$. Here $E_i$ and $E_{f,n}$ are the initial and final energies, unequal if there is an exchange of quanta (when $n\neq 0$). If there is no direct coupling between asymptotic wave functions, the transition amplitude is given by the "on-the-energy-shell" element of the operator $VG_F(E^+)V$ [15,26]:

$$t_{f,n\leftarrow i}(E)=\langle\langle\phi_{f,n}|VG_F(E^+)V|\phi_i\rangle\rangle. \tag{11}$$

The $\langle\langle\cdots\rangle\rangle$ mean that integration has to be done on both space and time. $V$ is the time-dependent coupling. $G_F(E^+)$ is the Green operator defined by

$$G_F(E^+)=\lim_{\epsilon\to 0}[E+i\epsilon-H_F]^{-1}. \tag{12}$$

However, a discretization of the spectrum of energies is possible if Siegert [27] boundary conditions are imposed. This can be done in an explicit manner by requiring the scattering wave function to be of outgoing character in both asymptotic regions. This can also be done by complex rotating the coordinate [28]. This produces a localization of the wave function, so that now the boundary conditions are the same as for a bound state. The elements of the set of discrete eigenvalues $E_\alpha$ are complex and called quasienergies. They can be written $E_\alpha=\Lambda_\alpha-i\Gamma_\alpha/2$. It is important to mention that if $\Phi_\alpha$ is a solution, $\exp[im\omega t]\,\Phi_\alpha=\Phi_{\alpha,m}$ is also a solution of quasienergy $E_\alpha+m\omega$. Although the solutions of the time-dependent Schrödinger equation issued from both functions are identical, all solutions of the eigenvalue equation with both $m$ and $\alpha$ as indices are needed to write the Green operator $G_F(E^+)$. This is due to the fact that the eigenvalue equation is solved in the extended space. The exponential $\exp[im\omega t]$ is not a phase factor in that space but a basis function and this affects the eigenvalue. Disregarding the continuous part of the spectrum of eigenvalues the Green operator is, in this context,

$$G_F(E)=[E-H_F]^{-1}=\sum_\alpha\sum_m\frac{|\Phi_{\alpha,m}\rangle\rangle\,\langle\langle\Phi_{\alpha,m}|}{E-(\Lambda_\alpha-i\Gamma_\alpha/2+m\omega)}. \tag{13}$$

The limiting operation is not necessary since there are no longer singularities along the real axis. Equations (11) and (13) have been used previously [16,26,29] to calculate transition probabilities. In the present context this expression of the Green operator is all we need to discuss the poles in the complex energy or frequency domains. With the moderate amplitude of oscillation used here, Table I shows that the first four over-barrier resonances have their energies little affected by the modulation. This means that we could equally well use the Green operator $G_F^0(E)=[E-H_F^0]^{-1}$ in the expression of the transition amplitude, where $H_F^0$ is the Floquet Hamiltonian in the extended space, but without the time-dependent barrier modulation. This is of considerable help in giving a meaning to each complex energy or frequency derived from the pole calculations.

## VI. POLES IN THE ENERGY AND FREQUENCY PLANES

The pole structure of the scattering amplitudes is entirely contained in the denominator of the Green operator.

### A. Poles in the energy plane: Explanation of the replica structure

The first application of the general expression of the transition amplitude will be to the replicas observed in Fig. 1. Table I has shown that the poles in the energy plane associated with the replicas are simply shifted down by one quantum and conserve the imaginary part of their parent resonance. This a simple consequence of looking at the zeros of the denominator of the Green operator given by

$$E_{\alpha,m}=\Lambda_\alpha+m\omega-i\frac{\Gamma_\alpha}{2}. \tag{14}$$

This relation shows how the energy poles depend on the frequency. It shows also how, from a given quasienergy, an infinite set of quasienergies can be generated by the addition or substraction of quanta. The three replicas shown in Fig. 1 correspond to the poles $E_{\alpha,-1}$, with $1\leqslant\alpha\leqslant 3$. For a larger modulation amplitude, replicas for $m=-2,-3,\ldots$ should appear. This was observed in a previous investigation of this phenomenon [13]. In the present case efficient transmission occurs either as a result of the resonance tunneling phenomenon already present in the static case or as the result of the absorption of one quantum to benefit from this same phenomenon.

### B. Poles in the frequency plane

The frequencies which make the denominator of the Green operator zero are given by

$$\omega_{\alpha,m} = m^{-1}[E - \Lambda_\alpha] + i\frac{\Gamma_\alpha}{2m}. \quad (15)$$

This expression shows how the frequency poles depend on the incident energy. Let us consider the resonant structure of Fig. 2 for an incident energy $E_{inc}$ equal to 10 eV. The peaks labeled (a), (b), (c), and (d) are interpreted in Table II as leading to the overbarrier resonances of energies $\Lambda_\alpha$ by the absorption of one quantum. According to Eq. (15) applied with $m=-1$ there should be complex frequency poles given by

$$\omega_{\alpha,-1} = \Lambda_\alpha - E - i\frac{\Gamma_\alpha}{2}. \quad (16)$$

On the other hand, the peaks labeled $(\alpha)$, $(\beta)$, and $(\gamma)$ correspond to the absorption of, respectively, four, three, and two quanta to reach the first overbarrier resonance of energy $\Lambda_1$. The complex frequency poles should be given by Eq. (15), with $\alpha=1$ and $m$ equal to $-4$, $-3$, and $-2$. The last two columns of the upper part of Table II confirm fully this analysis. The column marked "pole (num.)" gives the numerical evaluations of the poles while the column marked "pole (an.)" gives the estimates obtained from Eq. (15), with the use of the data given in Table I. An interesting property of the poles associated with multiquantum processes is that their imaginary part is divided by the number of quanta. The narrowing effect predicted by Eq. (15) is visible on Fig. 2.

We turn now to the case with an incident energy equal to 20 eV. The general formula given in Eq. (15) is now to be applied with $m=1$ and $\alpha$ equal 1 to 4, giving

$$\omega_{\alpha,1} = E - \Lambda_\alpha + i\frac{\Gamma_\alpha}{2}. \quad (17)$$

The lower part of Table II gives the poles obtained numerically and their reconstruction from the primitive data of Table I. It is to be noted that in all these pole calculations the most efficient procedure is to look at the zeros of the inverse of $t_n^{(3)}$, where $n$ is the number of absorbed quanta explaining a given feature in Fig. 2 (given also in column 2 of Table II). This is to be understood in the algebraic sense—that is, with $n$ positive for all peaks produced with $E_{inc}=10$ eV and $n$ negative for those produced with $E_{inc}=20$ eV.

Finally let us consider an incident energy of the form $E_{inc}=\Lambda_\alpha+p\omega$ for a given value of $\alpha$—say, 1—and $p=-1$ to $-4$. Whatever the value of $p$, there is in the sum giving the Green operator a term with $\alpha=1$ and $m=p$. The complex frequency poles are given by

$$\omega_{1,p} = p^{-1}\left[\Lambda_1 + p\omega - \left(\Lambda_1 - i\frac{\Gamma_1}{2}\right)\right] = \omega + i\frac{\Gamma_1}{2p}. \quad (18)$$

Table III confirms that again the width of a frequency pole can be the width of an energy pole divided by an integer.

TABLE III. The incident energy (column 2) is a resonance energy shifted down by a number of quanta (column 1), with $\omega=1.35$ eV. According to Eq. (17), the pole in the frequency plane has an imaginary part which is that of the parent resonance energy divided by the number of quanta. All energies and frequencies are in eV.

| $p$ | $\Lambda_1+p\omega$ | Pole | $-\Gamma_1/2p$ |
|---|---|---|---|
| −1 | 10.0110 | $1.3489-i0.08566$ | 0.08566 |
| −2 | 8.6610 | $1.3500-i0.04230$ | 0.04283 |
| −3 | 7.3110 | $1.3500-i0.02863$ | 0.02855 |
| −4 | 5.9605 | $1.3500-i0.02156$ | 0.02141 |

## VII. CONCLUSIONS

The expression which is the basis of the search for the poles in the complex energy or frequency planes is of general applicability in scattering situations involving a periodic coupling or perturbation provided there is free motion in the asymptotic regions. Any structure observed when a transition probability is measured or calculated as a function of the frequency of the coupling could be assigned to the existence of poles in the complex frequency plane. Although the case examined here implies a rather weak amplitude of modulation which leads to an easy identification of the meaning of the poles, the expression for the Green operator at the basis of this study is valid for arbitrary values of the parameters of the model. It shows in particular that the determination of the poles from the scattering amplitudes is a possible route to the complex Floquet quasienergies, which bypasses the resolution of the Floquet eigenvalue equation.

## ACKNOWLEDGMENTS

R.L. thanks Arne Keller for drawing his attention to the work of Hagmann [14] and for useful discussions. Part of this work was done during a visit of R.L. to the Technion, Haifa, Israel.

[1] E. Merzbacher, *Quantum Mechanics* (Wiley, New York, 1970).
[2] C. Cohen-Tannoudji, B. Diu, and F. Laloë, *Mécanique Quantique* (Hermann, Paris, 1973).
[3] M. Büttiker and R. Landauer, Phys. Rev. Lett. **49**, 1739 (1982).
[4] M. Büttiker and R. Landauer, Phys. Scr. **32**, 429 (1985).
[5] J. A. Støvneng and E. H. Hauge, J. Stat. Phys. **57**, 841 (1989).
[6] I. Gilary, N. Moiseyev, S. Rahav, and S. Fishman, J. Phys. A **36**, L409 (2003).
[7] T. C. L. G. Sollner, W. D. Goodhue, P. E. Tannenwald, C. D. Parker, and D. D. Peck, Appl. Phys. Lett. **43**, 588 (1983).
[8] H. Drexler, J. S. Scott, S. J. Allen, K. L. Campman, and A. C. Gossard, Appl. Phys. Lett. **67**, 2816 (1995).
[9] G. S. Vieira, S. J. Allen, P. S. S. Guimarães, K. L. Campman,

and A. C. Gossard, Phys. Rev. B **58**, 7136 (1998).
[10] R. Tsu and L. Esaki, Appl. Phys. Lett. **22**, 562 (1972).
[11] L. L. Chang, L. Esaki, and R. Tsu, Appl. Phys. Lett. **24**, 593 (1974).
[12] D. Sokolovski, J. Phys. C **21**, 639 (1988).
[13] C. Pérez del Valle, R. Lefebvre, and O. Atabek, Phys. Rev. A **59**, 3701 (1998).
[14] M. J. Hagmann, Appl. Phys. Lett. **66**, 789 (1995).
[15] U. Peskin and N. Moiseyev, Phys. Rev. A **49**, 3712 (1994).
[16] I. Vorobeichik and N. Moiseyev, J. Phys. B **31**, 645 (1998).
[17] J. Z. Kaminski, Z. Phys. D: At., Mol. Clusters **16**, 153 (1990).
[18] P. K. Tien and J. P. Gordon, Phys. Rev. **129**, 647 (1963).
[19] M. Wagner, Phys. Rev. B **49**, 16544 (1994).
[20] Wenjun Li and L. E. Reichl, Phys. Rev. B **60**, 15732 (1999).
[21] R. A. Sacks and A. Szöke, Phys. Rev. A **40**, 5614 (1989).
[22] R. Lefebvre, J. Mol. Struct.: THEOCHEM **493**, 117 (1999).
[23] In their study of the transmission by an oscillating barrier, A. Pimpale, S. Holloway, and R. J. Smith, [J. Phys. A **24**, 3533 (1991)] ensure time matching only at $t=0$. This produces a formula which is nothing but the transmission by a static barrier.
[24] J. R. Taylor, *Scattering Theory* (Wiley, New York, 1972).
[25] G. Floquet, Ann. Sci. Ec. Normale Super. **12**, 47 (1983).
[26] U. Peskin and N. Moiseyev, J. Chem. Phys. **99**, 4590 (1993).
[27] A. F. J. Siegert, Phys. Rev. **56**, 750 (1939).
[28] N. Moiseyev, Phys. Rep. **302**, 211 (1998).
[29] I. Vorobeichik, R. Lefebvre, and N. Moiseyev, Europhys. Lett. **41**, 111 (1998).